Title

Controllable Multigeometry Nanoparticles via Cooperative Assembly of Amphiphilic Diblock Copolymer Blends with Asymmetric Architectures

Journal

ACS Nano, 12(2)

ISSN

1936-0851

Authors

Wang, Zhikun
Wang, Hongbing
Cheng, Meng
et al.

Publication Date

2018-02-27

DOI

10.1021/acsnano.7b07777

Peer reviewed

Controllable multi-geometry nanoparticles via cooperative assembly of amphiphilic diblock copolymer blends with asymmetric architectures

Zhikun Wang[1], Hongbing Wang[1], Meng Cheng[1], Chunling Li[1,2], Roland Faller[3], Shuangqing Sun[1,2*], Songqing Hu[1,2*]

[1]*College of Science and* [2]*Key Laboratory of New Energy Physics & Materials Science in Universities of Shandong, China University of Petroleum (East China), 266580 Qingdao, Shandong, China*

[3]*Department of Chemical Engineering, UC Davis, 95616 Davis, California, USA*

Abstract

Multi-geometry nanoparticles with high complexity in composition and structure have attracted significant attention for enhanced functionality. We assess a simple but versatile strategy to construct hybrid nanoparticles with sub-divided geometries through the cooperative assembly of diblock copolymer blends with asymmetric architectures. We report the formation of multi-compartmental, vesicular, cylindrical, and spherical structures from pure AB systems. Then, we explore the assemblies of binary AB/AC blends, where the two incompatible, hydrophobic diblock copolymers sub-divide into self-assembled local geometries, and the complexity of the obtained morphologies increases. We expand the strategy to ternary AB/AC/AD systems by tuning the effect of phase separation of different hydrophobic domains on the surface or internal region of the nanoparticle. The kinetic control of the co-assembly in the initial stage is crucial for controlling the final morphology. The interactions of copolymers with different block lengths and

chemistries enable the stabilization of interfaces, rims and ends of sub-domains in the hybrid multi-geometry nanoparticles. With further exploration of size and shape, the dependence of local geometry on the volume fraction is discussed. We show an efficient approach for controllable multi-geometry nanoparticle construction that will be useful for multifunctional and hierarchical nanomaterials.

Keywords: Cooperative assembly; diblock copolymer blends; multi-geometry nanoparticles

INTRODUCTION

In pursuing increasingly nano-sized objects with large compositional and geometrical complexity, one goal is bridging the gap between simple assemblies and sophisticated structural control.[1] Amphiphilic block copolymers that exhibit a rich interplay of multiple chemically distinct building blocks have demonstrated increasing complexity via solution supramolecular assembly.[2-4] In single chemistry (*e.g.*, diblock, triblock, comb- and star-like) copolymer solution suspensions, the nanostructure geometry can be controlled precisely by changing copolymer length, concentration and solvent selectivity, by external stimuli and additives, or by changing the solvent processing kinetic pathway.[2-11] Beyond the considerable success in single-copolymer nanoparticles with simple geometries such as spheres, cylinders and vesicles, recent attention has focused on the impact of multiphase particles or hierarchical assemblies with higher degree of complexity on optical, electronic and biomedical properties.[12-15] To this end, three or more polymer blocks are required so that the micellar core and the corona of self-assembled nanoparticles will vary in both composition and geometry.[16] An emerging promising approach is

the cooperative assembly of block copolymer blends, which introduces a second level of hierarchy through intermolecular block interactions in addition to block-solvent and intramolecular block interactions.[17-19] Through a unique design with respect to block architecture, chemistry and solvent property, block copolymer blends can be successfully directed to self-organize into nanostructures with complex geometries.[20-21]

The ability to kinetically trap different copolymers into nanoparticles provides an excellent opportunity to construct complex, multi-geometry nano-objects for multifunctional and hierarchical materials.[22-29] For blends of identical block lengths but different block chemistry, we have previously reported a versatile strategy for the preparation of spherical and cylindrical multi-compartment micelles with controllable core and corona structures.[30] By controlling the block length and chemistry, one can design nanostructures with hybrid geometries such as disk-sphere or disk-cylinder polymeric nanoparticles.[19] This strategy has focused on the cooperative assembly of block copolymer blends with various segregation degrees that lead to different locations and morphologies in multi-geometry nanoparticles.[24,31-33] Only few studies have considered block copolymers with similar molecular weights and relative block fractions, because it is experimentally difficult to perform solution self-assembly of block copolymer blends with well-defined parameter ranges of structure and chemistry. A systematic understanding of controlling the polymorphism of multiphase nanostructures with compositional and geometrical complexity remains a challenge.[1-8]

Here we develop a straightforward mixing strategy for the solution co-assembly of diblock copolymer blends that allows precise tuning of micelle and patch geometries (Figure 1, route for

binary geometries). We start from classical micelle polymorphs such as spheres (S), cylinders (C), vesicles/lamellae (V/L) and multi-compartmental systems (M). Then we explore new morphologies by combining different geometries. Multi-geometry nano-objects are obtained through the combination of sub-domains with specific geometries and degrees of segregation.[19,34] We show that novel multi-geometry nanostructures can be constructed in blends of diblock copolymers by tuning the relative block lengths and volume fractions of different copolymers. For this complex problem, we use dissipative particle dynamics (DPD) which has been widely used for modelling physical phenomena at relatively large time and length scales. The three systems of focus include pure AB, binary AB/AC and ternary AB/AC/AD, in which A is hydrophilic and B/C/D are incompatible but all hydrophobic. Blocks B/C/D share the same solvent selectivity to avoid interface driven arrangement.[30] Each diblock copolymer molecule consists of 20 linearly bonded beads. Figure 2a shows an example of the symmetric building blocks $A_{10}B_{10}$.

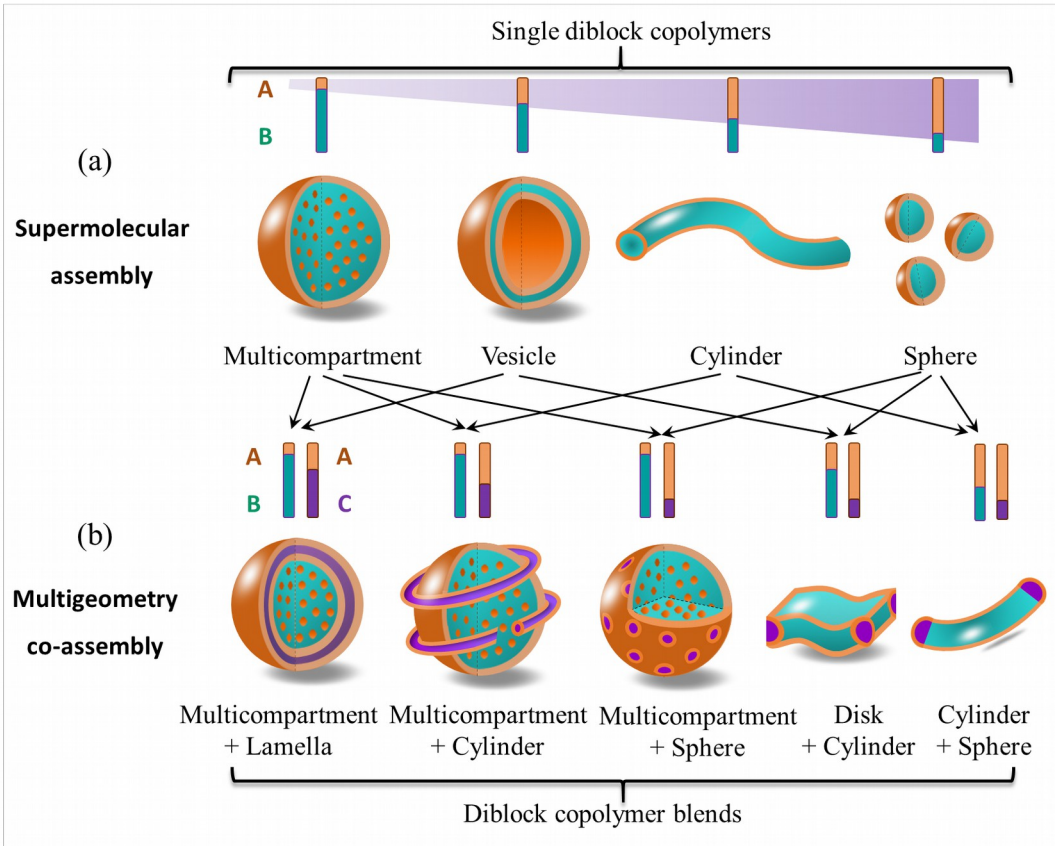

Figure 1. Schematic design for multi-geometry nanoparticles from diblock copolymer blends. (a) Multi-compartment (M), vesicle/lamella (V/L), cylinder (C), and sphere (S) micelles from single diblock copolymers with different hydrophilic/hydrophobic (A/B) block length ratios through desired solution assembly. (b) Binary multi-geometry micelles (M-L, M-C, M-S, D(disk)-C, and C-S) with two distinct domains obtained through cooperative assembly of diblock copolymers AB and AC in solution. The block length ratios of AB and AC are carefully selected for a specific geometry.

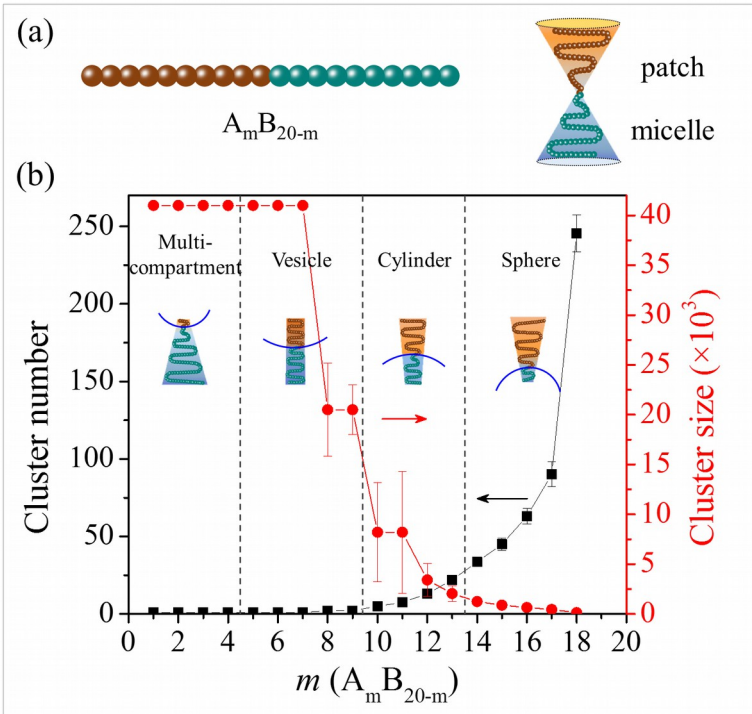

Figure 2. Cluster analysis of the pure AB system as a function of relative chain length m in A_mB_{20-m} (volume fraction ϕ_{AB} = 15%). The four regions indicate a morphological evolution of the micelle from multi-compartment to vesicle, cylinder and sphere.

RESULTS AND DISCUSSION

We first discuss the solution assembly of linear AB diblock copolymers into a variety of nanostructures where A forms the corona and B the cores (Figure 2b). The corona chain length m in A_mB_{20-m} controls micelle polymorphs to decrease the interface tension and total free energy by adjusting both intra- (self-segregation degree) and inter- (amphiphilic repulsion) molecular interactions.[4] A morphological evolution of the self-assembling micelles from M to V, C, and S is observed with increasing m. The dependence of aggregation state on m has been characterized by monitoring cluster number and cluster size (bead number in cluster). Moreover, the threshold

ratios for these nanostructures are predicted to be 5:15, 10:10 and 14:6, respectively, which quantitatively relates the micelle geometry to block lengths. To visualize the structural details of the 4 typical micelles, we address their assembly processes in Supporting Information (SI), Figure S1. Independent of geometry, the copolymers aggregate into a single micelle for $m < 8$, otherwise several small clusters are obtained and the number of clusters increases. The average cluster size (bead number in cluster) scales with the inverse of the number of clusters. Detailed structural analysis yields for increasing *m*, the size of hydrophilic cores in the multi-compartment micelle increases, the hydrophobic shell of the vesicle decreases and an overall shape change from cylindrical vesicle to spherical vesicle is observed. The lengths of cylindrical micelles gradually decrease and spherical micelles are obtained. The overall micelle morphology is controlled by the block lengths. Block-block enthalpic interactions influence the entropy of polymer domains. A longer hydrophobic block favors the location and alignment of copolymers at the micelle/solvent interface, since a loss in conformational entropy contributes to the aggregation of copolymers by overcoming the loss in polymer translational entropy. The block lengths dominate the compatibility of copolymers with respect to interface tension and drives the collapse of micelles at a long hydrophilic block, and thereby leads to changes in cluster number and size.

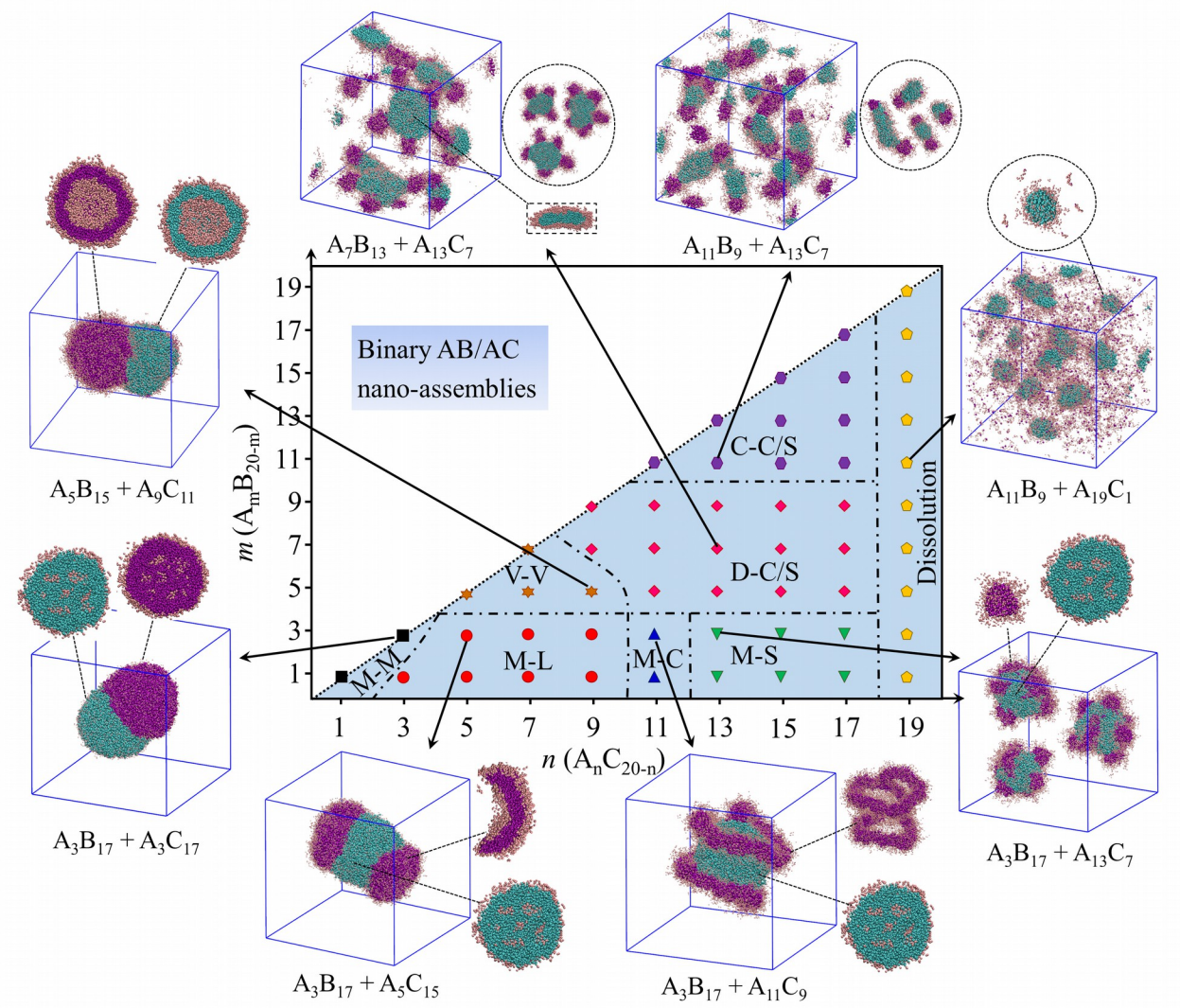

Figure 3. Morphology diagram of the AB/AC system as a function of m in A_mB_{20-m} and n in A_nC_{20-n} ($\phi_{AB} = \phi_{AC} =$ 7.5%). Arrows in the diagram indicate the typical morphologies of various types of hybrid nanoparticles. Pairwise capital letters indicate hybrid binary nanostructures from the combination of multi-compartment, vesicle, disk, cylinder, and sphere geometries. "Dissolution" indicates that AB copolymers form clusters and AC copolymers totally dissolve. Color scheme: brown-A, cyan-B, purple-C.

For multi-geometry nanoparticles, we explored the possibility to manipulate multiple morphologies via the co-assembly of binary AB/AC blends using precisely controlled block

lengths (Figure 3). The obtained hybrid micelles contain parts of M, V, L, C or S morphologies, and are formed through blending and attaching two unlike copolymers that segregate into sub-domains of distinct geometry and chemistry. 8 typical morphologies are obtained.

We first focus on M favoring copolymers ($m < 5$ in A_mB_{20-m}) which tend to form porous cores in hybrid nanoparticles due to their large hydrophobicity. (1) A hybrid M-M morphology (Janus) is obtained by the combination of two incompatible but architecturally similar copolymers, e.g., A_3B_{17} + A_3C_{17}, which both favor porous aggregations. (2) A hybrid M-L morphology (multi-caped) is obtained by the combination of M and V favoring copolymers, e.g., A_3B_{17} + A_5C_{15}, in which a L-type patch is formed around the M-type core through interface-driven assembly. Also, a "spreading-first" phenomenon is observed for copolymers of A_nC_{20-n} (n ranges from 3 to 9) on A_1B_{19} core as a single lamellar patch, and a "clustering-first" phenomenon is observed for copolymers of A_nC_{20-n} (n ranges from 5 to 9) on A_3B_{17} core as multiple lamellar patches (SI, Figure S2a,b). The spreading of copolymers on A_1B_{19} micelles reduces the interfacial energy due to the particularly high hydrophobicity of A_1B_{19} copolymers, while the clustering of copolymer caps on A_3B_{17} cores can be attributed to the truncation effect of the micelle surface on the vesicle favoring copolymers. (3) A hybrid M-C morphology (spiral patch) is obtained by the combination of M and C favoring copolymers, e.g., A_3B_{17} + $A_{11}C_9$, in which a cylindrical micelle wraps the M-type core in a spiral morphology. (4) A hybrid M-S morphology (satellite patch) is obtained by the combination of M and S favoring copolymers, e.g., A_3B_{17} + $A_{15}C_5$, in which small clusters are scattered on the surface of the M-type core. The increase of n in A_nC_{20-n} leads to the increase of cluster number but decrease of cluster size, which highlights the effect of interfacial

patches on the distribution of clusters (SI, Figure S2c).

Copolymers that favor V-type morphology ($5 \leq m < 10$ in A_mB_{20-m}) tend to form bilayer structures, vesicles or disks, in the hybrid nanoparticles. (5) A hybrid V-V morphology (vesicle-on-vesicle) is obtained from two V favoring copolymers, e.g., A_5B_{15} + A_9C_{11}. The hybrid vesicle can be in a simple Janus-like mode or an alternatively connection mode. The interfacial curvature of AC bilayers can be slightly altered by changing n in A_nC_{20-n} (SI, Figure S2d). (6) When V and C/S favoring copolymers are mixed, e.g., A_7B_{13} + $A_{13}C_7$, a hybrid D(disk)-C/S morphology is obtained, in which vesicles are cut into disks and cylinder or sphere "tentacles" that adopt a higher interfacial curvature after assemblies stabilize the disk edges. The assembly of a bilayer disk is difficult since the rim is a high energy defect, and thus a stabilizer is needed when the co-assembly is initiated. With proper design of block lengths, the sizes of the disk and "tentacle" can be controlled (SI, Figure S2e). (7) Moreover, when both copolymers favor C or S ($n \geq 11$, $m \geq 11$), a hybrid C-C/S morphology (Janus-like), e.g., $A_{11}B_9$ + $A_{13}C_7$, can be obtained. Again, the lengths of the hybrid nanoparticles depend on the block lengths of components (SI, Figure S2f). (8) The dissolution region in Figure 3 indicates that $A_{19}B_1$ copolymers do not aggregate due to large solubility. Overall, the hybrid nanoparticles have been constructed through interface-driven separation of core and patch copolymers. Tunable clustering of core or patch sub-domains is achievable for hybrid nanoparticles such as M-L, M-S, D-C/S and C-C/S. Detailed molecular interaction modes leading to the morphology differences in these hybrid nanoparticles are illustrated in Figure S3.

In addition to inherent geometrical restrictions by block length, the sub-domain dimension of

the designed binary nanoparticles can be defined by the volume fraction, ϕ, of copolymers. The morphological evolutions of the assembled nanoparticles from AB/AC systems through the defined blending pathway are shown and fully discussed in Figure S4. We also analyzed the effect of ϕ_{AC} on clustering and enthalpic interaction of copolymers (Figure 4). M-L and M-C hybrid nanoparticles have a constant clustering of the M-type core and a dominant dimension increase (i.e., core/patch contact) of the patches, e.g., cluster analysis of A_3B_{17} + A_7C_{13} and A_3B_{17} + A_7C_{13}. M-S, D-C/S and C-S hybrid nanoparticles show a large ϕ_{AC}-dependent clustering (number and size) that the hydrophobic core splits into a number of small detached clusters, e.g., cluster analysis of A_3B_{17} + $A_{15}C_5$, A_7B_{13} + $A_{11}C_9$, A_7B_{13} + $A_{15}C_5$, and $A_{11}B_9$ + $A_{15}C_5$. The evolutions of average energy E_{AB+AC}/N_{AB+AC} and E_{AB+AC}/N_{AB+AC} versus increasing ϕ_{AC} further demonstrate that the interfacial interactions of these hybrid nanoparticles are gradually weakened. Both, morphology and quantitative analysis (Figures S4, 4), indicate that patches with large volume fraction stabilize the interfaces, especially edges in disk and ends in cylinder, and serve as truncation effect for the control of cluster dimension.[19,23] Moreover, as the current calculation is conducted in a relatively high concentration, we provide a better insight by reducing the concentration to 5% or even lower (SI, Figure S5 and S6). Except for unavoidable size decrease at lower concentration, the assembly of copolymers (both pure AB and binary AB/AC systems) exhibit consistent principle with those at high concentration. Thus, the directed co-assembly strategy has significant potential in the preparation of soft templates with controlled geometry and dimension.

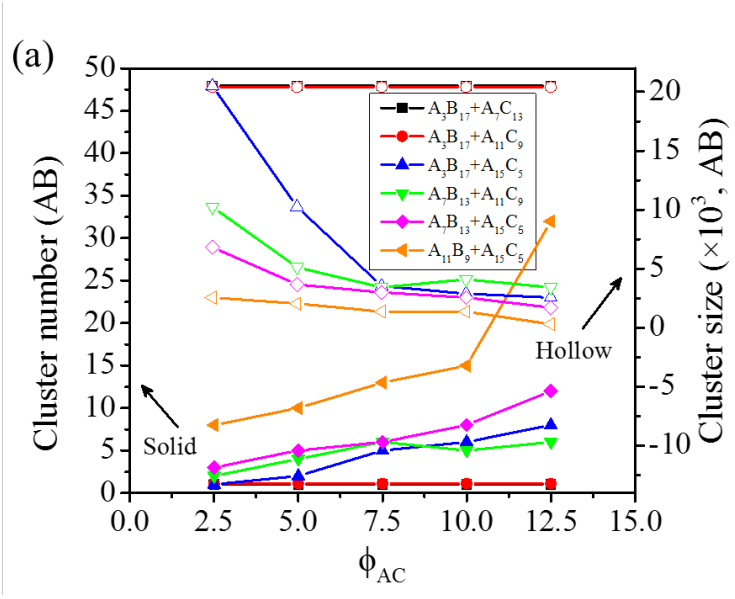
(a)
Cluster number (AB)
Cluster size (×10^3, AB)
ϕ_AC
Solid
Hollow
A3B17+A7C13
A3B17+A11C9
A3B17+A15C5
A7B13+A11C9
A7B13+A15C5
A11B9+A15C5

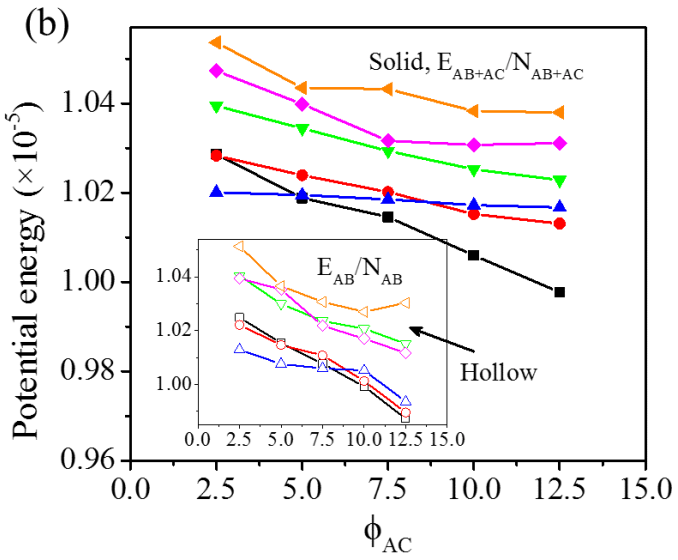

Figure 4. Clustering behavior (a) and potential energy (b) evolution of hybrid nanoparticles as a function of volume fraction of AC (ϕ_{AC}) in an AB/AC system (ϕ_{AB} = 7.5%). Copolymer blends of A_3B_{17} + A_7B_{13}, A_3B_{17} + $A_{11}B_9$, A_3B_{17} + $A_{15}B_5$, A_7B_{13} + $A_{11}B_9$, A_7B_{13} + $A_{15}B_5$, and $A_{11}B_9$ + $A_{15}B_5$ indicate hybrid nanoparticles of M-L, M-C, M-S, D-C, D-S, and C-S, respectively. Solid and hollow symbols in (a) indicate cluster number and cluster size, respectively, while in (b) indicate averaged energies AB+AC and AB.

The success in multi-geometry co-assembly from binary AB/AC blends relies on surface as well as internal organization of nanoparticles with proper block length ratio and concentration of polymers.[20-21,35] The self-segregation degree of copolymers and selectivity of solvent for the blocks provides the kinetic control of the assembly so that unlike hydrophobic blocks will contribute to the proper multi-geometry nanoparticle confinement.[36-37] The initial stage of the co-assembly is crucial for the final morphology, e.g., disks in D-S type nanoparticles are not easily obtained if the vesicles are initially closed before stabilizing with rim-attached spheres. An additional critical aspect for the co-assembly strategy is the incompatibility of different

hydrophobic blocks, which determines either attachment or detachment of patches on micelles.[30] The repulsive parameter in the present study (a_{BC} = 45) adopts a moderate repulsion between blocks B and C, thus AC patches are properly adsorbed on micelles. The above effects, including segregation degree, selectivity of solvent and incompatibility of hydrophobic blocks, explain why the assembled nanoparticles phase separate into multi-geometric polymorphs. Figure S7 to S11 in SI exhibit further evaluations on how to select the repulsive parameters to obtain the specific nano-structures in this work. These discussions reveal a much broader world for the preparation of novel and versatile nano-structures based on the co-assembly strategy of copolymer blends.

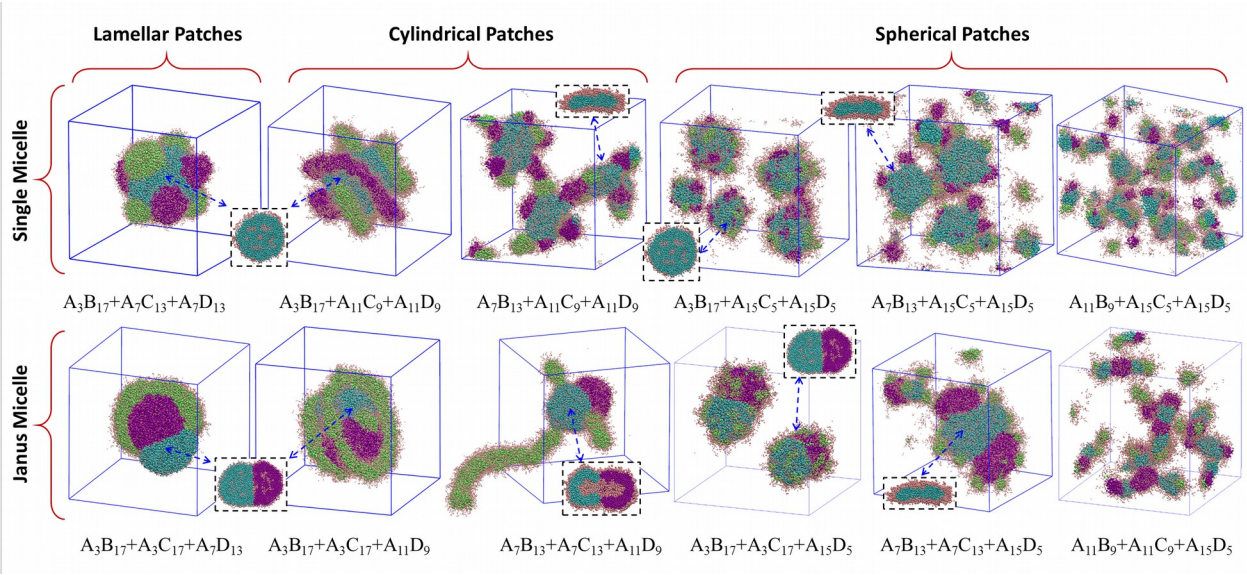

Figure 5. Controlled morphologies with hybrid lamellar, cylindrical or spherical patches from ternary blends with two architecturally identical diblock copolymers. The nanoparticles are classified into mixed-patch/pure-core and pure-patch/mixed-core categories. For single core (identical block lengths C and D), polymorph types of M-L-L, M-C-C, D-C-C, M-S-S, D-S-S, and C-S-S are shown in the upper row, left to right. For mixed

(Janus) core (identical block lengths B and C), M-M-L, M-M-C, V-V-C, M-M-S, D-D-S, and C-C-S are obtained successively in lower row, left to right. Color scheme: brown-A, cyan-B, purple-C, green-D.

Through this blending assembly strategy, we extend the construction of multi-geometry nanoparticles by adding a third diblock copolymer AD. Obviously, the ternary system contains a high level of complexity for co-assembly of copolymers. We observe similar co-assembly behavior (clustering and phase separation) and concentration dependence in the binary except for more precise modifications on the phase separation of hydrophobic domains. Under the same solution assembly condition, a series of ternary hybrid nanoparticles from the combination of M, V/L, C, and S micelles are obtained. We focus on the manipulation of surface and internal organizations in the assembled nanoparticles by tuning the block lengths, n_A, of AB, AC and AD for more complex geometries. Tunable composition and geometry of either hybrid patch or hybrid core domains can be achieved. Through systematic exploration, we divide the possible ternary multi-geometries into four critical categories: lamellar patches, cylindrical patches, spherical patches, and hybrid patches. Figure 5 shows the assembled nanoparticles when two of the three copolymers are incompatible but have the same architecture. Formation of various overall or local morphologies in these nanostructures through ternary co-assembly, as well as concentration related dimension control, is shown in Figures S12, S13. Figure 6 shows the assembled nanoparticles of three incompatible and architecturally different copolymers, as well as the concentration related dimension control. We produce highly complex hybrid patches by organizing three different geometries within a single nanoparticle. During co-assembly, different copolymers combine to stabilize the micelle interface, rim or end areas to limit high energy

defects and reduce the free energy of the system. Kinetic control of the assembly process together with precise regulation of the hydrophobic block interactions dominate the local equilibrium of polymer chains within the nanoparticles. A summary of the multi-geometry nanoparticles is shown in Figure S14. Overall, ternary nanoparticles with more complex core or patch geometries need more precise control on the geometries and sizes of different domains, which can be defined by the architecture and volume fraction of copolymers.

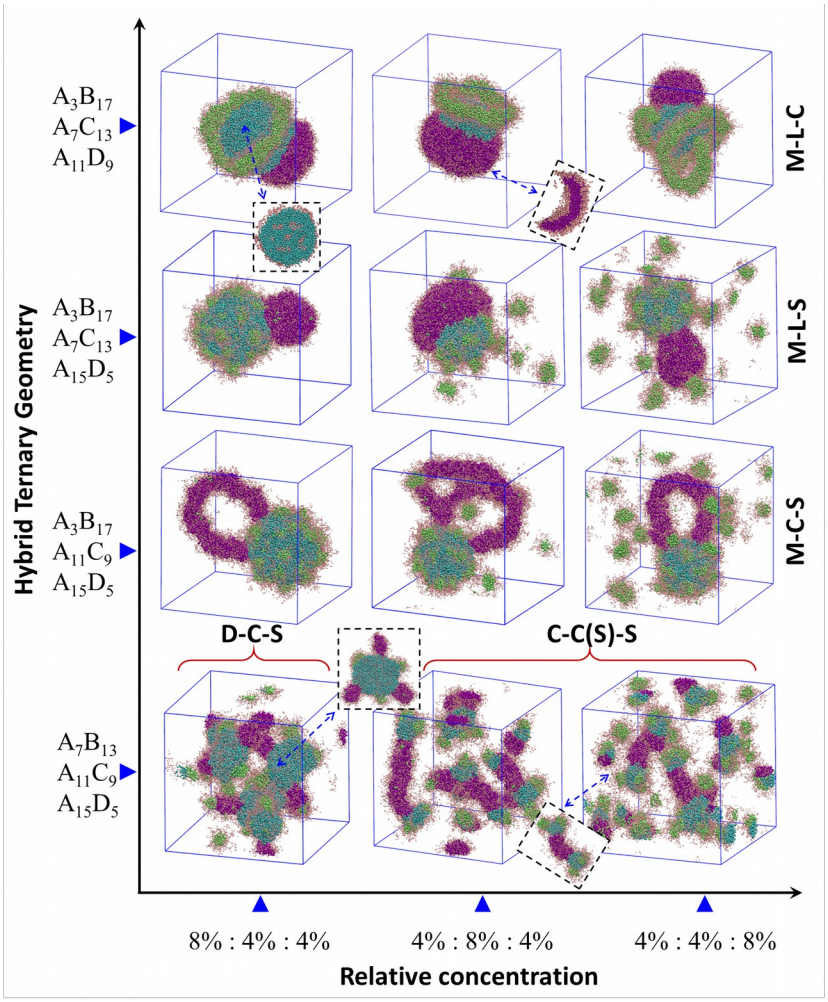

Figure 6. Controlled morphologies of ternary blends with three architecturally different diblock copolymers. M-L-C, M-L-S, M-C-S, D-C-S, and C-C(S)-S are obtained through the combination of multi-compartment.

lamellar, cylindrical and spherical favorable copolymers. The influence of the relative concentration of the three copolymers on the nanoparticle geometry is illustrated. The horizontal axis indicates the relative concentration of copolymers (ϕ_{AB} : ϕ_{AC} : ϕ_{AD}) in ternary systems. Color scheme: brown-A, cyan-B, purple-C, green-D.

CONCLUSIONS

We propose a molecular strategy for the construction of multi-geometry nanoparticles with designed surface or internal morphologies from the cooperative assembly of diblock copolymer blends with defined block lengths. Starting from the self-assemblies of classical geometries, such as sphere, cylinder, vesicle/lamella and multi-compartmental units, formed by pure AB diblock copolymer systems, we explore the blend assembly of these geometries in binary AB/AC and ternary AB/AC/AD systems. A number of binary hybrid nanoparticles with combined geometries of M-M, M-L, M-C, M-S, V-V, D-C/S, and S-C/S have been obtained by blending of AB and AC. We determined the molecular design parameters (e.g., relative chain lengths) for the different structures. Also, the construction of more complex nanoparticles with mixed-surface/pure-core or pure-surface/mixed-core geometries from ternary AB/AC/AD systems were explored. Further control of size or shape of sub-domains in hybrid nanoparticles can be achieved by tuning the volume fraction. This strategy shows great potential for design and preparation of multi-functional soft materials through kinetic control of solution co-assembly of binary, ternary or higher order blends. Further investigations on the property characterizations and potential applications of these multi-geometry nanoparticles are planned.

METHODS

We use dissipative particle dynamics (DPD)[38] which employs a soft repulsive potential and a momentum-conserving thermostat to control pairwise particle interactions for the exploration of the co-assembly of diblock copolymer blends. As a coarse-grained method, DPD has been used to investigate physical phenomena of soft materials, where repeat units or cluster of molecules are grouped together and represented by a single bead, for larger time and length scales than typical molecular dynamics (MD).[39-41] The time evolution is governed by Newton's equation of motion $m\,\mathrm{d}\boldsymbol{v}_i/\mathrm{d}t = \boldsymbol{f}_i$, where $\boldsymbol{v}_i$ and $\boldsymbol{f}_i$ indicate the velocity and force on the ith bead with mass m at time t. The velocity-Verlet algorithm has been used for the integration of the equation of motion.[38] In the simulations, the force on a bead i at position $\boldsymbol{r}_i$ surrounded by beads $j \neq i$ at $\boldsymbol{r}_j$ (distance vector $\boldsymbol{r}_{ij} = \boldsymbol{r}_i - \boldsymbol{r}_j$ and unit vector $\boldsymbol{e}_{ij} = \boldsymbol{r}_{ij}/r_{ij}$ with $r_{ij} = |\boldsymbol{r}_{ij}|$) is a sum of the components of the conservative force $\boldsymbol{F}^{\mathrm{C}}$, the dissipative force $\boldsymbol{F}^{\mathrm{D}}$, the random force $\boldsymbol{F}^{\mathrm{R}}$, as well as the bond stretching force $\boldsymbol{F}^{\mathrm{S}}$, $\boldsymbol{f}_i = (\boldsymbol{F}^{\mathrm{C}}{}_{ij} + \boldsymbol{F}^{\mathrm{D}}{}_{ij} + \boldsymbol{F}^{\mathrm{R}}{}_{ij} + \boldsymbol{F}^{\mathrm{S}}{}_{ij})$, where the sum runs over all beads j within a cutoff radius r_c. The conservative interaction force is described by $\boldsymbol{F}^{\mathrm{C}}{}_{ij} = \alpha_{ij}\omega^{\mathrm{C}}(r_{ij})\boldsymbol{e}_{ij}$, where α_{ij} is the maximum repulsion between beads i and j, the weight function $\omega^{\mathrm{C}}(r_{ij}) = 1 - r_{ij}/r_c$ for $r_{ij} < r_c$ and $\omega^{\mathrm{C}}(r_{ij}) = 0$ for $r_{ij} \geq r_c$. The dissipative force is given by $\boldsymbol{F}^{\mathrm{D}}{}_{ij} = -\gamma\omega^{\mathrm{D}}(r_{ij})(\boldsymbol{v}_{ij} \cdot \boldsymbol{e}_{ij})\boldsymbol{e}_{ij}$, where $\boldsymbol{v}_{ij} = \boldsymbol{v}_i - \boldsymbol{v}_j$ and γ indicates the dissipative strength. The random force is $\boldsymbol{F}^{\mathrm{R}}{}_{ij} = \sigma\omega^{\mathrm{R}}(r_{ij})\xi_{ij}(\mathrm{d}t)^{1/2}\boldsymbol{e}_{ij}$, where ξ_{ij} is a random variable of zero-mean Gaussian distribution with unit variance. σ is the noise defined as $\sigma = (2k_{\mathrm{B}}T\gamma)^{1/2}$, where k_{B} is the Boltzmann constant and T is temperature. Dissipative and random forces together act as a thermostat. The bond stretching force is given by $\boldsymbol{F}^{\mathrm{S}}{}_{ij} = C\boldsymbol{r}_{ij}$.

We use the dissipative parameter $\gamma = 4.5$ and the stiffness constant $C = -4$. In $\boldsymbol{F}^{\mathrm{C}}$, the repulsive parameters α_{ii} between all like species are chosen to be 25, while for block-block and block-

solvent the interactions are chosen as $\alpha_{AB} = \alpha_{AC} = \alpha_{AD} = \alpha_{BC} = \alpha_{BD} = \alpha_{CD} = 45$, $\alpha_{AW} = 26$, and $\alpha_{BW} = \alpha_{CW} = \alpha_{DW} = 100$, respectively, where A, B, C, D, and W indicate the beads of the three diblock copolymers (A-hydrophilic, B/C/D-hydrophobic and incompatible) and water (W). The cutoff radius, bead mass, temperature, and thermal energy are set as unit system, that is $r_c = m = T = k_BT = 1$. The characteristic time scale for the simulation is $\tau = r_c(m/k_BT)^{1/2}$. The box size is $(45r_c)^3$ with a bead number density of $3/r_c^3$. The system contains a total of 273 375 beads. Periodic boundary conditions are employed in all three directions. We set the time step $\Delta t = 0.05\tau$. The simulations start from randomly dispersed diblock copolymer blends in solution. 1.0×10^6 to 3.0×10^6 time steps are used to ensure that the systems reach equilibrium.

AUTHOR INFORMATION

Corresponding Authors

*E-mail: sunshuangqing@upc.edu.cn

*E-mail: songqinghu@upc.edu.cn

Notes

The authors declare no competing financial interest.

ACKNOWLEDGMENTS

The authors acknowledge the financial supports from the National Natural Science Foundation of China (51201183 and 51501226), and Fundamental Research Funds for the Central Universities (14CX02221A, 16CX06023A, 16CX05017A and 17CX05023).

REFERENCES

(1) Lunn, D. J.; Finnegan, J. R.; Manners, I., Self-assembly of "patchy" nanoparticles: a versatile approach to functional hierarchical materials. *Chem. Sci.* **2015**, *6* (7), 3663-3673.

(2) Tritschler, U.; Pearce, S.; Gwyther, J.; Whittell, G. R.; Manners, I., 50th Anniversary Perspective: Functional Nanoparticles from the Solution Self-Assembly of Block Copolymers. *Macromolecules* **2017**, *50* (9), 3439-3463.

(3) Moughton, A. O.; Hillmyer, M. A.; Lodge, T. P., Multicompartment Block Polymer Micelles. *Macromolecules* **2012**, *45* (1), 2-19.

(4) Mai, Y.; Eisenberg, A., Self-assembly of block copolymers. *Chem. Soc. Rev.* **2012**, *41* (18), 5969-5985.

(5) Gröschel, A. H.; Müller, A. H., Self-assembly concepts for multicompartment nanostructures. *Nanoscale* **2015**, *7* (28), 11841-11876.

(6) Zhang, Q.; Lin, J.; Wang, L.; Xu, Z., Theoretical modeling and simulations of self-assembly of copolymers in solution. *Prog. Polym. Sci.* **2017**, *75*, 1-30.

(7) Wyman, I. W.; Liu, G., Micellar structures of linear triblock terpolymers: Three blocks but many possibilities. *Polymer* **2013**, *54* (8), 1950-1978.

(8) Holder, S. J.; Sommerdijk, N. A. J. M., New micellar morphologies from amphiphilic block copolymers: disks, toroids and bicontinuous micelles. *Polym. Chem.* **2011**, *2* (5), 1018-1028.

(9) Groschel, A. H.; Muller, A. H. E., Self-assembly concepts for multicompartment nanostructures. *Nanoscale* **2015**, *7* (28), 11841-11876.

(10) Stuart, M. A. C.; Huck, W. T.; Genzer, J.; Müller, M.; Ober, C.; Stamm, M.; Sukhorukov, G. B.; Szleifer, I.; Tsukruk, V. V.; Urban, M., Emerging applications of stimuli-responsive polymer

materials. *Nat. Mater.* **2010**, *9* (2), 101-113.

(11) Xu, J.; Yang, Y.; Wang, K.; Li, J.; Zhou, H.; Xie, X.; Zhu, J., Additives Induced Structural Transformation of ABC Triblock Copolymer Particles. *Langmuir* **2015**, *31* (40), 10975-10982.

(12) Kuzyk, A.; Schreiber, R.; Fan, Z.; Pardatscher, G.; Roller, E.-M.; Hogele, A.; Simmel, F. C.; Govorov, A. O.; Liedl, T., DNA-based self-assembly of chiral plasmonic nanostructures with tailored optical response. *Nature* **2012**, *483* (7389), 311-314.

(13) Borys, N. J.; Walter, M. J.; Huang, J.; Talapin, D. V.; Lupton, J. M., The Role of Particle Morphology in Interfacial Energy Transfer in CdSe/CdS Heterostructure Nanocrystals. *Science* **2010**, *330* (6009), 1371-1374.

(14) Geng, Y.; Dalhaimer, P.; Cai, S.; Tsai, R.; Tewari, M.; Minko, T.; Discher, D. E., Shape effects of filaments versus spherical particles in flow and drug delivery. *Nat. Nanotechnol.* **2007**, *2* (4), 249-255.

(15) Sing, C. E.; Zwanikken, J. W.; Olvera de la Cruz, M., Electrostatic control of block copolymer morphology. *Nat. Mater.* **2014**, *13* (7), 694-698.

(16) Löbling, T. I.; Borisov, O.; Haataja, J. S.; Ikkala, O.; Gröschel, A. H.; Müller, A. H. E., Rational design of ABC triblock terpolymer solution nanostructures with controlled patch morphology. *Nat. Commun.* **2016**, *7*, 12097.

(17) Christian, D. A.; Tian, A.; Ellenbroek, W. G.; Levental, I.; Rajagopal, K.; Janmey, P. A.; Liu, A. J.; Baumgart, T.; Discher, D. E., Spotted vesicles, striped micelles and Janus assemblies induced by ligand binding. *Nat. Mater.* **2009**, *8*, 843.

(18) Zhu, J.; Zhang, S.; Zhang, F.; Wooley, K. L.; Pochan, D. J., Hierarchical Assembly of Complex

Block Copolymer Nanoparticles into Multicompartment Superstructures through Tunable Interparticle Associations. *Adv. Funct. Mater.* **2013**, *23* (14), 1767-1773.

(19) Zhu, J.; Zhang, S.; Zhang, K.; Wang, X.; Mays, J. W.; Wooley, K. L.; Pochan, D. J., Disk-cylinder and disk-sphere nanoparticles via a block copolymer blend solution construction. *Nat. Commun.* **2013**, *4* 2297.

(20) Vyhnalkova, R.; Müller, A. H. E.; Eisenberg, A., Control of Morphology and Corona Composition in Aggregates of Mixtures of PS-b-PAA and PS-b-P4VP Diblock Copolymers: Effects of Solvent, Water Content, and Mixture Composition. *Langmuir* **2014**, *30* (44), 13152-13163.

(21) Vyhnalkova, R.; Müller, A. H. E.; Eisenberg, A., Control of Corona Composition and Morphology in Aggregates of Mixtures of PS-b-PAA and PS-b-P4VP Diblock Copolymers: Effects of pH and Block Length. *Langmuir* **2014**, *30* (17), 5031-5040.

(22) Pochan, D. J.; Zhu, J.; Zhang, K.; Wooley, K. L.; Miesch, C.; Emrick, T., Multicompartment and multigeometry nanoparticle assembly. *Soft Matter* **2011**, *7* (6), 2500-2506.

(23) Chen, Y.; Zhang, K.; Wang, X.; Zhang, F.; Zhu, J.; Mays, J. W.; Wooley, K. L.; Pochan, D. J., Multigeometry Nanoparticles: Hybrid Vesicle/Cylinder Nanoparticles Constructed with Block Copolymer Solution Assembly and Kinetic Control. *Macromolecules* **2015**, *48* (16), 5621-5631.

(24) Gao, C.; Wu, J.; Zhou, H.; Qu, Y.; Li, B.; Zhang, W., Self-Assembled Blends of AB/BAB Block Copolymers Prepared through Dispersion RAFT Polymerization. *Macromolecules* **2016**, *49* (12), 4490-4500.

(25) Cheng, L.; Lin, X.; Wang, F.; Liu, B.; Zhou, J.; Li, J.; Li, W., Well-Defined Polymeric Double Helices with Solvent-Triggered Destruction from Amphiphilic Hairy-Like Nanoparticles.

Macromolecules **2013**, *46* (21), 8644-8648.

(26) Jeon, S.-J.; Yi, G.-R.; Yang, S.-M., Cooperative Assembly of Block Copolymers with Deformable Interfaces: Toward Nanostructured Particles. *Adv. Mater.* **2008**, *20* (21), 4103-4108.

(27) Xu, J.; Wang, K.; Liang, R.; Yang, Y.; Zhou, H.; Xie, X.; Zhu, J., Structural Transformation of Diblock Copolymer/Homopolymer Assemblies by Tuning Cylindrical Confinement and Interfacial Interactions. *Langmuir* **2015**, *31* (45), 12354-12361.

(28) Han, S. H.; Pryamitsyn, V.; Bae, D.; Kwak, J.; Ganesan, V.; Kim, J. K., Highly asymmetric lamellar nanopatterns via block copolymer blends capable of hydrogen bonding. *ACS Nano* **2012**, *6* (9), 7966-7972.

(29) Palanisamy, A.; Guo, Q., Large Compound Vesicles from Amphiphilic Block Copolymer/Rigid-Rod Conjugated Polymer Complexes. *J. Phys. Chem. B* **2014**, *118* (44), 12796-12803.

(30) Wang, Z.; Sun, S.; Li, C.; Hu, S.; Faller, R., Controllable multicompartment morphologies from cooperative self-assembly of copolymer-copolymer blends. *Soft Matter* **2017**, *13* (35), 5877-5887.

(31) Liu, M.; Qiang, Y.; Li, W.; Qiu, F.; Shi, A.-C., Stabilizing the Frank-Kasper Phases via Binary Blends of AB Diblock Copolymers. *ACS Macro Lett.* **2016**, *5* (10), 1167-1171.

(32) Yan, N.; Sheng, Y.; Liu, H.; Zhu, Y.; Jiang, W., Templated Self-Assembly of Block Copolymers and Morphology Transformation Driven by the Rayleigh Instability. *Langmuir* **2015**, *31* (5), 1660-1669.

(33) Cambridge, G.; Gonzalez-Alvarez, M. J.; Guerin, G.; Manners, I.; Winnik, M. A., Solution self-assembly of blends of crystalline-coil polyferrocenylsilane-block-polyisoprene with crystallizable polyferrocenylsilane homopolymer. *Macromolecules* **2015**, *48* (3), 707-716.

(34) Löbling, T. I.; Borisov, O.; Haataja, J. S.; Ikkala, O.; Gröschel, A. H.; Müller, A. H., Rational design

of ABC triblock terpolymer solution nanostructures with controlled patch morphology. *Nat. Commun.* **2016**, *7*.

(35) Kamps, A. C.; Fryd, M.; Park, S.-J., Hierarchical Self-Assembly of Amphiphilic Semiconducting Polymers into Isolated, Bundled, and Branched Nanofibers. *ACS Nano* **2012**, *6* (3), 2844-2852.

(36) Wang, X.; Guerin, G.; Wang, H.; Wang, Y.; Manners, I.; Winnik, M. A., Cylindrical block copolymer micelles and co-micelles of controlled length and architecture. *Science* **2007**, *317* (5838), 644-647.

(37) Cui, H.; Chen, Z.; Zhong, S.; Wooley, K. L.; Pochan, D. J., Block copolymer assembly via kinetic control. *Science* **2007**, *317* (5838), 647-650.

(38) Groot, R. D.; Warren, P. B., Dissipative particle dynamics: Bridging the gap between atomistic and mesoscopic simulation. *J. Chem. Phys.* **1997**, *107* (11), 4423-4435.

(39) Yan, L.-T.; Popp, N.; Ghosh, S.-K.; Böker, A., Self-Assembly of Janus Nanoparticles in Diblock Copolymers. *ACS Nano* **2010**, *4* (2), 913-920.

(40) Alexeev, A.; Uspal, W. E.; Balazs, A. C., Harnessing Janus Nanoparticles to Create Controllable Pores in Membranes. *ACS Nano* **2008**, *2* (6), 1117-1122.

(41) Wang, Z.; Gao, J.; Ustach, V.; Li, C.; Sun, S.; Hu, S.; Faller, R., Tunable Permeability of Cross-Linked Microcapsules from pH-Responsive Amphiphilic Diblock Copolymers: A Dissipative Particle Dynamics Study. *Langmuir* **2017**, *33* (29), 7288-7297.

For Table of Contents use only:

Controllable multi-geometry nanoparticles via cooperative assembly of amphiphilic diblock copolymer blends with asymmetric architectures

Zhikun Wang[1], Hongbing Wang[1], Meng Cheng[1], Chunling Li[1,2], Roland Faller[3], Shuangqing Sun[1,2*], Songqing Hu[1,2*]

[1]*College of Science and* [2]*Key Laboratory of New Energy Physics & Materials Science in Universities of Shandong, China University of Petroleum (East China), 266580 Qingdao, Shandong, China*

[3]*Department of Chemical Engineering, UC Davis, 95616 Davis, California, USA*

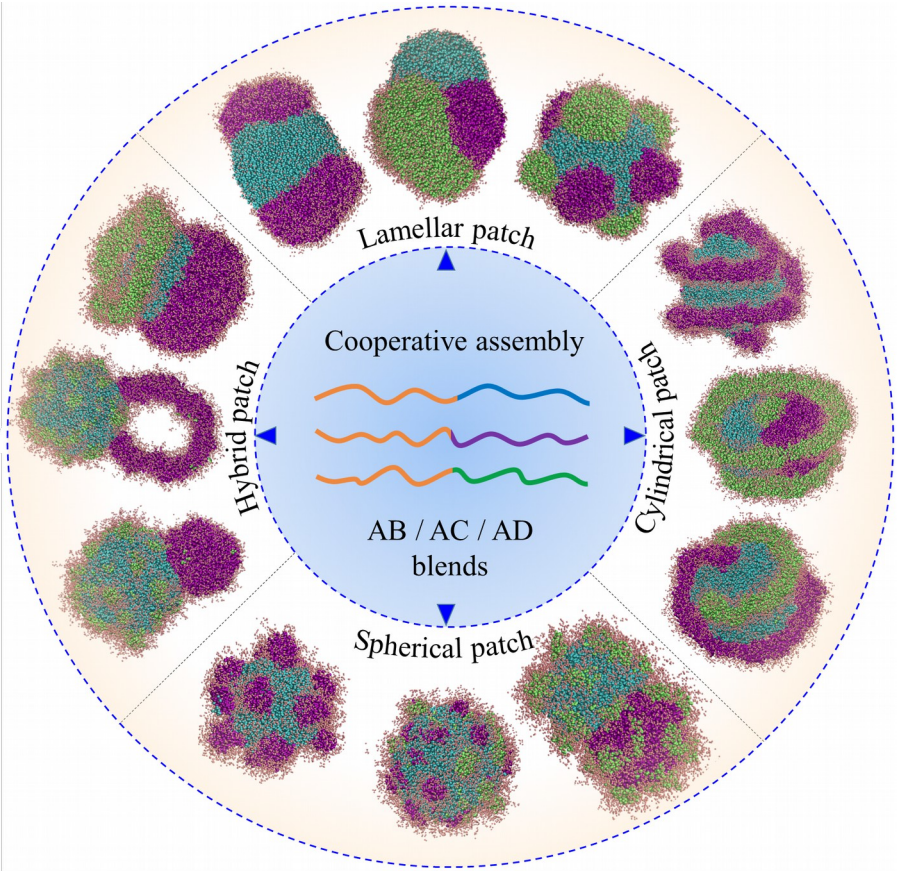
Lamellar patch
Cooperative assembly
Hybrid patch
Cylindrical patch
AB / AC / AD
blends
Spherical patch